

We are IntechOpen, the world's leading publisher of Open Access books Built by scientists, for scientists

6,900

Open access books available

186,000

International authors and editors

200M

Downloads

Our authors are among the

154

Countries delivered to

TOP 1%

most cited scientists

12.2%

Contributors from top 500 universities



WEB OF SCIENCE™

Selection of our books indexed in the Book Citation Index
in Web of Science™ Core Collection (BKCI)

Interested in publishing with us?
Contact book.department@intechopen.com

Numbers displayed above are based on latest data collected.
For more information visit www.intechopen.com



A Competitive Approach for Designing Multi-Antenna Cognitive Access Networks^{*}

E. Baccarelli, M. Biagi, N. Cordeschi,
T. Patriarca and V. Polli
*"Sapienza", University of Rome
Info-Com Dept.
Italy*

1. Introduction to the cognitive MIMO radio paradigm

Cognitive radio has recently shown its great potential for 4th-Generation wireless local access networks (i.e., 4GWLANS) and attracted worldwide interest in academics, industry and standardization activities (Glisic, 2006). The US Federal Communication Commission (FCC, 2003) has issued a notice of public rule-making and order regarding cognitive radio technologies. The Defense Advanced Research Project Agency (DARPA, 2001) launched the 'next generation (XG) communication program' to develop new technologies to dynamically manage the radio spectrum. The US Army has also been researching 'adaptive spectrum exploitation' (ASE) for real-time spectrum management in the battlefield (Lee, 2001). The US National Science Foundation (NSF) has recently launched the 'Programmable Wireless Networking' (ProWin) program focused on adaptive, agile, cognitive radios and networking. On the standardization side, the IEEE 802.22 working group is elaborating on the use of TV bands for spectral-agile wireless regional access networks (WRANs) (Cordiero et al., 2005; IEEE 802.22, 2005). Basically, cognitive radio is capable of ascertaining its operating environment and adapting to real-time conditions of its (localized) wireless channel, including the ability to sense spectrum-usage by neighbouring devices, change operating frequency band, adjust radiated power and modify transmission parameters (Mitola, 1999; Haykin, 2005; Mangold et al., 2004; Zheng & Cao, 2005). Such an intelligent and agile use of the spectrum resource is expected to improve the spectrum-access capability of emerging 4GWLANS (Glisic, 2006; Butler & Webb, 2006; IEEE 802.22, 2005; Chow et al., 2007).

However, wireless access capacity may be also improved significantly by resorting to multi-antenna (i.e., MIMO) architectures that allow exploiting the spatial dimension of the

^{*} This work has been partially supported by the Italian National Project: Wireless multiplatform mimo active access networks for QoS-demanding multimedia Delivery (WORLD), under grant number 2007R989S.

underlying access system via SDMA (Shad et al., 2001; Paulraj et al., 2003). From this point of view, the MIMO paradigm offers, indeed, several important capabilities (such as spatial degree of freedom, spatial diversity, multiple-access interference (MAI) mitigation) that may be suitably exploited for increasing the overall access efficiency of 4GWLANS (Glisic, 2006; Paulraj et al., 2003). However, in order to fully avail of these spatial capabilities offered by the MIMO paradigm in a flexible and agile way, a still open key-question concerns the design of asynchronous, scalable and self-configuring SDMA policies able to meet the QoS-requirements advanced by (battery-powered nomadic) users.

In principle, this flexibility may be attained by merging the cognitive paradigm with the MIMO one, thus giving rise to the cognitive MIMO radio paradigm. In fact, the cognitive concept directly leads to the development of distributed, scalable, and flexible radio access networking architectures by resorting to an opportunistic and (possibly) competitive real-time management of the available radio-resource, that, in turns, may be suitably modelled via the formal tool of Game Theory (Fudenberg & Tirole, 1991, Chaps 16, 24).

1.1 Previous works on competitive cognitive-inspired access

Specifically, distributed power-control in wireless access networks by exploiting Game Theory is tackled in (MacKenzie & Wicker, 2001). A game-theoretic approach is also pursued in (Palomar et al., 2003) for dealing with power-allocation in single-user MIMO systems in the presence of imperfect channel estimation. The paper (Altman & Altman, 2003) examines the general application of the super-modular games to the distributed power-control, while the contribution in (Goodman & Mandayam, 2000) considers an application scenario wherein the accessing radios attempt to maximize a suitable function of their throughput and leads to the conclusion that the underlying game converges to a Nash Equilibrium (NE). Later, (Saraydar et al., 2002) point out that the game considered in (Goodman & Mandayam, 2000) is, indeed, a super-modular game. The contribution in (Sung & Wong, 2003) focuses on a (somewhat modified) version of the single-cell distributed power-control game that is based on the concept of nonlinear group pricing. Applications of Game Theory to fair-efficient admission control are presented in (Virapanicharoen & Benjpolakaul, 2004), while the whole topic of competitive flow-control and distributed routing is discussed in (Kannan & Iyengar, 2004; Altman et al. 2002).

Game theoretic approaches for agile spectrum sharing have been recently developed in (Fattahi et al., 2007; Xing et al., 2007; Wang & Brown, 2007). Specifically, (Fattahi et al., 2007) focus on the design of a coordinated mechanism for allocating time and frequency slots to competing users that are capable to self-reconfigure their terminals via cross-layer strategies. (Xing et al., 2007) explore the price dynamics of a competitive market composed by (multiple) self-interested service providers that compete for potential customers by offering heterogeneous spectrum-agile networking technologies at different costs. (Wang & Brown, 2007) develop a public safety and commercial spectrum-sharing strategy that resorts to both agile network pricing and call admission control for the competitive maximization of the commercial revenue under low (e.g., upper limited) blocking-probability to public safety calls.

Overall, all the above cited works consider applications scenarios characterized by either single-antenna radios (i.e., they do not consider the spatial dimension), or single-user MIMO systems (i.e., they do not deal with the access problem), thus leaving open the question about potential access capability of the cognitive MIMO radio paradigm.

1.2 Proposed contributions and application scenarios

This chapter focuses on the competitive access in WLAN systems operating in an infrastructure-mode, where power-limited multi-antenna non-cooperative cognitive self-configuring radios attempt to join in uplink to a (possibly multi-antenna) access point (AP) (Fig. 1(a)). The target pursued by each radio is to maximize its own access information-throughput in the presence of both (Rayleigh-distributed) flat-fading and MAI induced by the other accessing terminals. For achieving this goal in a fully distributed and asynchronous way (i.e., in a non-cooperative way), each radio exploits its cognitive capability to 'learn' (i.e., estimate) both its own current MIMO faded uplink and the covariance matrix of the MAI induced by the other accessing radios. Thus, on the basis of these learned (i.e., acquired) context information, each radio proceeds to self-reconfigure its access policy by performing suitable power-allocation and (statistical) spatial-shaping of the radiated signals. This learning/self-configuring action is autonomously iterated by the accessing radios according to the general rules of the non-cooperative strategic games, until the overall Access Network (AN) converges to a stable operating state (e.g., the NE of the underlying game). We investigate the performance of this competitive and cognitive access policy under both best-effort and contracted-QoS access strategies.

Furthermore, we also consider the case when even the AP is cognitive, thus meaning that it attempts to learn and subtract the MAI contribution affecting the signal received by each accessing radio. Overall, the key-results of this work may be so summarized.

- First, the access strategy we present exploits both the spatial-dimension offered by the physical MIMO platform and the cognitive capability of the AN to maximize (in a competitive sense) the access throughput of each accessing radio. Interestingly, this goal is achieved without requiring radio synchronisation and/or peer-to-peer information-passing among the radio terminals (i.e., in a fully asynchronous and distributed way).
- Second, the proposed access strategy allows to implement both best-effort and contracted-QoS access policies, and it may also provide for multiple QoS classes. Interestingly enough, we anticipate that, when the QoS-requirements advanced by the radios are no sustainable by the AN, thus, the proposed access algorithm is able to self-move the operating point of the whole AN (e.g., the operating NE point) to the nearest sustainable one. This means that, besides the radio terminals, the overall AN we go to develop is, indeed, cognitive and self-configuring. Thus, it may be considered as an instance of active access network (Glisic, 2006; Chap.16).
- Finally, several numerical results corroborate the conclusion that the proposed cognitive and self-configuring AN is able to outperform conventional CSMA/CA/OFDMA/CDMA/TDMA-based no cognitive access systems in terms of both aggregate access throughput and access capacity, especially when the MAI experienced at the AP side is strong.

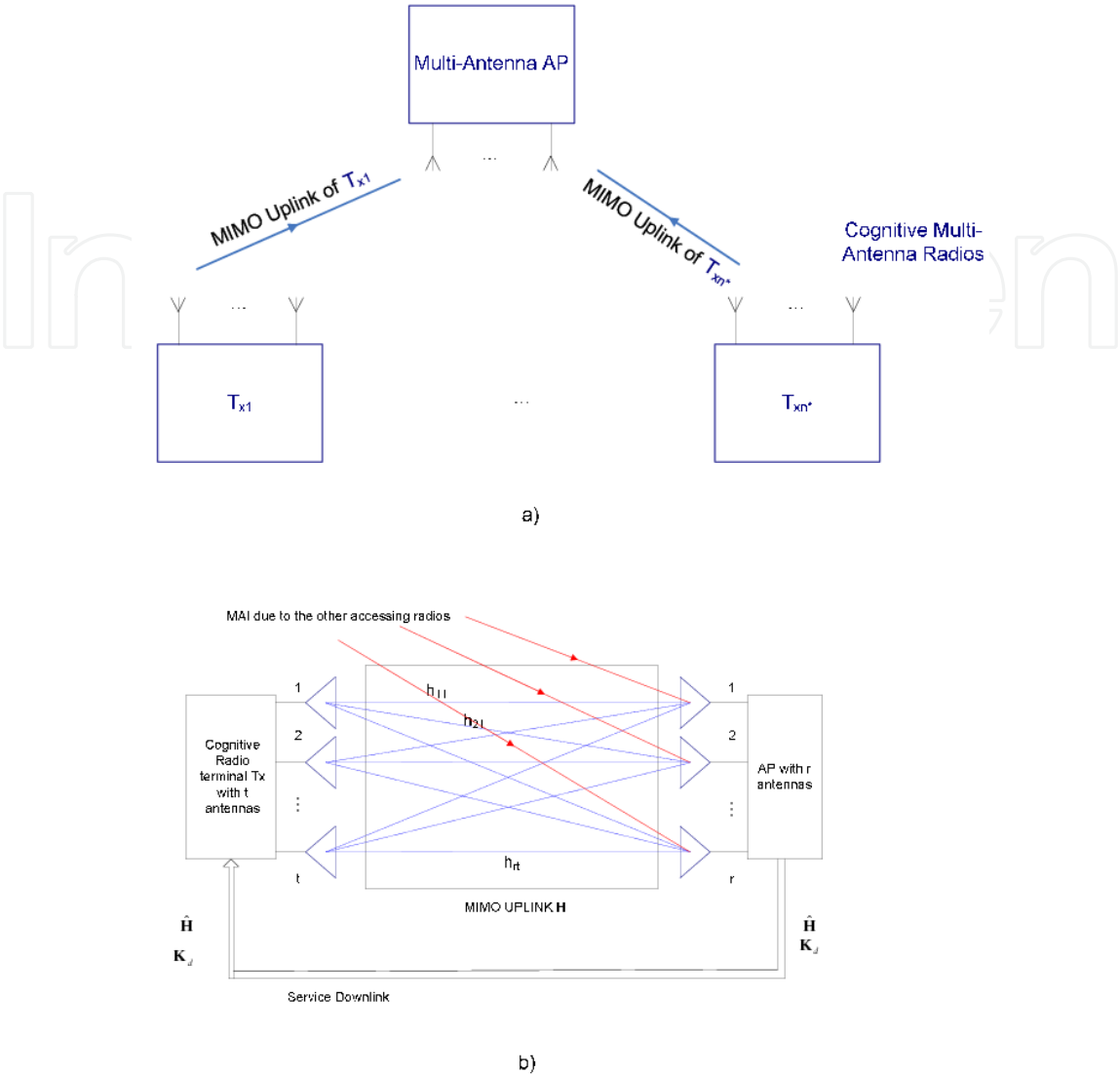


Fig. 1. (a) The considered multi-antenna local AN (b) Zoomed block diagram of the up-down links joining the radio terminal Tx to the AP

1.3 Organization of the chapter

The remainder of this work is organized as follows. After the system modelling of Section 2, Section 3 deals with the evaluation of the conveyed information throughput in wireless access networks affected by MAI. In Section 4 the optimized power-allocation and interference mitigation algorithms are presented. Thus, after shortly reviewing in Section 5 some Game Theory essentials, in Section 6 we propose a game-inspired access policy. Actual performance of the proposed access strategy in terms of access throughput and access capacity is tested in Section 6, while some conclusive remarks are drawn in Section 7. About the adopted notation, we anticipate that, capital letters indicate matrices, lower-case underlined symbols denote vectors, while characters overlined by arrow denote block-matrices and block-vectors. Furthermore, apexes $*$, T , \dagger , mean conjugation, transposition and conjugate-transposition respectively, while lowercase letters will be used for scalar

quantities. Furthermore, $\det[\mathbf{A}]$ and $\text{Tra}[\mathbf{A}]$ mean determinant and trace of the matrix $\mathbf{A} \triangleq [\underline{a}_1 \dots \underline{a}_m]$. Finally, \mathbf{I}_m is the $(m \times m)$ identity matrix, $\|\mathbf{A}\|_E$ is the Euclidean norm of the matrix \mathbf{A} , $\mathbf{A} \otimes \mathbf{B}$ is the Kronecker product of the matrix \mathbf{A} by matrix \mathbf{B} , $\mathbf{0}_m$ is the m -dimensional zero-vector, \lg denotes natural logarithm and $\delta(m,n)$ is the Kronecker delta.

2. The considered SDMA network-model

As previously anticipated, the application scenario we consider is the MIMO uplink of a packet-oriented WLAN, where $n^* \geq 2$ multi-antenna battery-powered radios attempt to simultaneously access to a (possibly multi-antenna) AP (Fig. 1(a)). Since the accessing radios are assumed non-cooperative, we begin to focus on the MIMO uplink joining a single radio Tx to the AP, thus considering the signals radiated by all other (n^*-1) accessing radios as (additive) MAI. The resulting (complex base-band equivalent) point-to-point MAI-impaired MIMO uplink is sketched in Fig. 1(b). Simply stated, this uplink is composed by an accessing radio Tx (equipped with $t \geq 1$ antennas) communicating to the AP (equipped with $r \geq 1$ antennas) via a MIMO channel impaired by both Rayleigh flat fading and additive MAI. Path gain h_{ji} from the transmit antenna i to the receive one j in Fig. 1(b) may be modelled as a complex zero-mean unit-variance proper complex random variable (r.v.) (Baccarelli & Biagi, 2003; Paulraj et al., 2003), and, for sufficiently spaced-apart antennas, the path gains $\{h_{ji} \in \mathbb{C}, 1 \leq j \leq r, 1 \leq i \leq t\}$ may be considered mutually uncorrelated (Paulraj et al., 2003). Furthermore, these gains h_{ji} may be also assumed time-invariant over $T \geq 1$ signalling periods, after which they change to new statistically independent values held for another T signalling period, and so on. The resulting 'block-fading' model well captures the main features of several frequency-hopping or packet based interleaved 4G systems, where each transmitted packet is detected independently of any other (Paulraj et al., 2003). Since the statistic features of the MAI in Fig. 1(b) depend on both WLAN topology and signals radiated by all accessing radios, it is reasonable to assume that these statistics remain constant over (at least) the whole packet duration. However, since both path gains h_{ji} and MAI statistics may change from a packet to another, we assume that radios and AP are not aware of them at the beginning of each transmitted packet, but they may exploit their cognitive capabilities to learn (i.e., acquire) them. For this purpose, according to the packet-oriented structure of the considered WLAN, we assume that the (coded and modulated) data-streams radiated in uplink by the transmit antennas of Fig. 1(b) are split into packets composed by $T \geq 1$ slots, where the first T_{L1} slots are used by the receiver (i.e., the AP) to 'learn' the MAI statistics (Section 2.1), the second T_{L2} slots are employed to 'learn' the path gains of the forward MIMO channel (Section 2.2), and the last $T_{\text{pay}} = T - T_{L1} - T_{L2}$ slots convey payload data (Section 2.3).

2.1 First learning phase

During the first learning phase, no signal is radiated by the Tx radio of Fig. 1(b), so as to allow the AP to learn the statistics of the MAI induced by all other accessing radios (Fig. 1(a)). Thus, the r -dimensional (complex column) vector collecting the outputs of the receive antennas at the AP side over the n -th slot of this first learning phase may be modelled as

$$\underline{y}(n) \triangleq \underline{\dot{d}}(n) \equiv \underline{\dot{v}}(n) + \underline{\dot{w}}(n), \quad 1 \leq n \leq T_{L1}. \quad (1)$$

In (1), $\underline{\dot{w}}(n)$ accounts for the receiver thermal noise, so that $\{\underline{\dot{w}}(n)\}$ may be modelled as a zero-mean, proper complex, spatially and temporally white sequence, with covariance matrix equal to

$$E\{\underline{\dot{w}}(n)(\underline{\dot{w}}(n))^{\dagger}\} = \mathcal{N}_0 \mathbf{I}_r \delta(m, n), \quad (1.1)$$

where \mathcal{N}_0 (Watt / Hz) is the thermal noise level. The component $\{\underline{\dot{v}}(n)\}$ in (1) accounts for the MAI induced by all other accessing radios, and thus it may be suitably modelled as a zero mean, temporally-white, spatially-colored Gaussian sequence (Paulraj et al., 2003), with covariance matrix $\mathbf{K}_v \triangleq E\{\underline{\dot{v}}(n)(\underline{\dot{v}}(n))^{\dagger}\}$ constant over (at least) a packet-transmission interval. However, since \mathbf{K}_v may change from a packet to another, it is reasonable to assume that both Tx and AP in Fig. 1(b) are not aware of the overall disturbance covariance matrix

$$\mathbf{K}_d \triangleq E\{\underline{\dot{y}}(n)(\underline{\dot{y}}(n))^{\dagger}\} \equiv \mathbf{K}_v + \mathcal{N}_0 \mathbf{I}_r, \quad (2)$$

at the beginning of each transmitted packet. Besides, since during this first learning phase the signal $\underline{\dot{y}}(n)$ in (1) received at the AP equates the MAI one $\underline{\dot{d}}(n)$, the AP may exploit its cognitive capabilities to learn \mathbf{K}_d . A very simple way to accomplish this task is suggested by the law of large numbers (Poor, 1994). By fact, this last guarantees that an unbiased and consistent (i.e., asymptotically exact) estimate $\tilde{\mathbf{K}}_d$ may be obtained via the following sample-average:

$$\tilde{\mathbf{K}}_d = \frac{1}{T_{L1}} \sum_{n=1}^{T_{L1}} E\{\underline{\dot{y}}(n)(\underline{\dot{y}}(n))^{\dagger}\}. \quad (3)$$

As already pointed out in (Baccarelli et al., 2007), we anticipate that the performance effects of (possible) mismatches between actual \mathbf{K}_d and its estimate $\tilde{\mathbf{K}}_d$ are not so critical, so that, in the sequel, we directly assume $\tilde{\mathbf{K}}_d = \mathbf{K}_d$. However, this assumption will be relaxed in Section 6.5, where the effects of possible mismatches are numerically tested.

2.2 Second learning phase

Goal of the second learning phase is to allow the accessing radio to perform the optimized shaping of the (deterministic) pilot streams $\{\tilde{x}_i(n), T_{L1} + 1 \leq n \leq T_{L1} + T_{L2}, 1 \leq i \leq t\}$ to be used to estimate the (a priori unknown) $(r \times t)$ uplink gains h_{ji} . Thus, the (sampled) signal $\tilde{y}_i(n)$ measured at the output of the j -th receive antenna of the AP node during this second learning phase may be modelled as (Paulraj et al., 2003)

$$\tilde{y}_j(n) = \frac{1}{\sqrt{t}} \sum_{i=1}^t h_{ji} \tilde{x}_i(n) + \tilde{d}_j(n), \quad T_{L1} + 1 \leq n \leq T_{L1} + T_{L2}, \quad (4)$$

where the overall disturbance $\tilde{d}_j(n)$ accounts for both MAI and thermal noise and exhibits the same statistics previously reported in (2). Therefore, the $(T_{L2} \times r)$ observations in (4) may be recast into the $(T_{L2} \times r)$ matrix $\tilde{Y} \triangleq [\tilde{y}_1 \dots \tilde{y}_r]$ given by

$$\tilde{Y} = \frac{1}{\sqrt{t}} \tilde{X}H + \tilde{D}, \quad (5)$$

where $\tilde{X} \triangleq [\tilde{x}_1 \dots \tilde{x}_t]$ is the $(T_{L2} \times t)$ matrix of the radiated pilot symbols in (4), $H \triangleq [h_1 \dots h_r]$ is the $(t \times r)$ matrix composed by the uplink gains $\{h_{ji}\}$ to be learned, and the $(T_{L2} \times r)$ matrix $\tilde{D} \triangleq [\tilde{d}_1 \dots \tilde{d}_r]$ collects the MAI-plus-noise terms $\tilde{d}_j(n)$ in (4).

Afterwards, observations \tilde{Y} in (5) are employed by the AP to 'learn' H via the computation of the corresponding minimum mean squared error (MMSE) matrix estimate $\hat{H} \triangleq E\{H|\tilde{Y}\}$. Thus, at step $n = T_{L1} + T_{L2}$ (i.e., at the end of the second learning phase), this matrix estimate \hat{H} is communicated back to the accessing radio via the service downlink of Fig. 1(b). A detailed analysis of the structure and performance of the estimator computing the set $\hat{h}_{ji} \triangleq E\{h_{ji}|\tilde{Y}\}$ of the $(r \times t)$ MMSE estimates of the MIMO uplink H in (5) may be found in (Baccarelli et al., 2007; Biagi, 2006). For our purposes, it suffices to stress that the pilot matrix \tilde{X} minimizing the total average squared estimation error:

$$\sigma_{tot}^2 \triangleq \sum_{j=1}^r \sum_{i=1}^t E\{\|\hat{h}_{ji} - h_{ji}\|^2\} = \sum_{j=1}^r \sum_{i=1}^t E\{\|\varepsilon_{ji}\|^2\}, \quad (5.1)$$

must meet the following relationship (Baccarelli & Biagi, 2003; Baccarelli et al., 2007):

$$K_d^{-1} \otimes \tilde{X}^\dagger \tilde{X} \equiv aI_{rt}, \quad (6)$$

where

$$a \triangleq \frac{T_{L2} \tilde{P}}{r} \text{Tra}\{K_d^{-1}\}, \quad (7)$$

and \tilde{P} (Watt) in (7) is the average power available at Tx radio for the transmission of the pilot signals in (4). Furthermore, it may be also proved (Baccarelli et al., 2007) that, when \tilde{X} meets the condition in (6), the resulting MMSE estimation errors $\{\varepsilon_{ji} \triangleq \hat{h}_{ji} - h_{ji}\}$ are mutually uncorrelated, zero-mean, and equidistributed proper complex Gaussian r.v.s, with variance

$$\sigma_{\varepsilon}^2 \triangleq E\{\|\varepsilon_{ji}\|^2\} = (1 + a/t)^{-1}. \quad (8)$$

2.3 Payload phase

On the basis of the available K_d and \hat{H} matrices and actual packet to be transmitted, the Tx radio of Fig. 1(b) suitable shapes the signal streams $\{\phi_i(n) \in \mathbb{C}^1, T_{L1} + T_{L2} + 1 \leq n \leq T, 1 \leq i \leq t\}$ to be radiated during the payload phase. Hence, the corresponding (sampled) signals $\{y_j(n) \in \mathbb{C}^1, T_{L1} + T_{L2} + 1 \leq n \leq T, 1 \leq j \leq r\}$ measured at the outputs of the receive antennas at the AP side may be modelled (Paulraj et al., 2003; Baccarelli et al., 2007) as

$$y_j(n) = \sqrt{\frac{\beta}{t}} \sum_{i=1}^t h_{ji} \phi_i(n) + d_j(n), \quad T_{L1} + T_{L2} + 1 \leq n \leq T, \quad (9)$$

where the sequence $d_j(n) \triangleq v_j(n) + w_j(n)$, $1 \leq j \leq r$, accounts for the overall disturbances (e.g., MAI plus thermal noise) experienced during the payload phase, $\beta \triangleq D^{-z}$ takes care of the path loss over a distance of D meters and z is the corresponding path-loss exponent. Therefore, after assuming that the transmitted streams meet the (usual) average power constraint

$$\frac{1}{t} \sum_{i=1}^t E\{\|\phi_i(n)\|^2\} \leq P, \quad (10)$$

the resulting SINR γ_j measured at the output of the j -th receive antenna at the AP side during the payload phase equates (equations (9), (10))

$$\gamma_j = aP/(\mathcal{N}_o + c_{jj}), \quad 1 \leq j \leq r, \quad (11)$$

where c_{jj} is the (j,j) -th entry of the MAI covariance matrix K_d in (2). Moreover, from (9) we also deduce that the $(r \times 1)$ column vector $\underline{y}(n) \triangleq [y_1(n) \dots y_r(n)]^T$ collecting the outputs of the r receive antennas over the n -th payload slot is linked to the $(t \times 1)$ column vector $\underline{\phi}(n) \triangleq [\phi_1(n) \dots \phi_t(n)]^T$ of the corresponding signals radiated by the accessing radio as in

$$\underline{y}(n) = \sqrt{\frac{\beta}{t}} \mathbf{H}^T \underline{\phi}(n) + \underline{d}(n), \quad T_{L1} + T_{L2} + 1 \leq n \leq T, \quad (12)$$

where $\{\underline{d}(n) \triangleq [d_1(n) \dots d_r(n)]^T, T_{L1} + T_{L2} + 1 \leq n \leq T\}$ is the temporally-white spatially-colored Gaussian sequence of disturbances with spatial covariance matrix still given by K_d . Furthermore, directly from (10) it follows that the $(t \times t)$ spatial covariance matrix

$\mathbf{R}_\phi \triangleq E\{\underline{\phi}(n)\underline{\phi}(n)^\dagger\}$ of the t -dimensional signal vector radiated during each by the Tx radio of Fig. 1(b) must meet the following power constraint:

$$\text{Tra}[\mathbf{R}_\phi] \triangleq E\{\underline{\phi}(n)^\dagger \underline{\phi}(n)\} \leq tP. \quad (13)$$

Finally, after stacking the T_{pay} observed vectors in (12) into the corresponding $(T_{\text{pay}}r \times 1)$ block vector $\underline{\tilde{y}} \triangleq [\underline{y}^T(T_{L1} + T_{L2} + 1) \dots \underline{y}^T(T)]^T$, we may compact the T_{pay} relationships (12) into the following one:

$$\underline{\tilde{y}} = \sqrt{\frac{\beta}{t}} [\mathbf{I}_{T_{\text{pay}}} \otimes \mathbf{H}]^T \underline{\tilde{\phi}} + \underline{\tilde{d}}, \quad (14)$$

where the (block) covariance matrix of the corresponding disturbance (block) vector in (14) $\underline{\tilde{d}} \triangleq [\underline{d}^T(T_{L1} + T_{L2} + 1) \dots \underline{d}^T(T)]^T$ is given by

$$E\{\underline{\tilde{d}}(\underline{\tilde{d}})^\dagger\} = \mathbf{I}_{T_{\text{pay}}} \otimes \mathbf{K}_d, \quad (15)$$

while the average Euclidean squared norm of the block vector $\underline{\tilde{\phi}} \triangleq [\underline{\phi}^T(T_{L1} + T_{L2} + 1) \dots \underline{\phi}^T(T)]^T$ of the transmitted random signals is constrained as (equation (10))

$$E\{\underline{\tilde{\phi}}^\dagger \underline{\tilde{\phi}}\} \leq T_{\text{pay}} tP. \quad (16)$$

3. Self-reconfiguration of the cognitive MIMO-radios

We pass now to introduce a suitable performance metric that allows the accessing radio of Fig. 1(b) to both ‘learn’ its current achieved performance and, possibly, self-reconfigure its access strategy for improving it. Specifically, the performance metric we consider is the Shannon capacity of the MIMO uplink, formally defined as

$$\mathcal{C}(\hat{\mathbf{H}}) \triangleq \sup_{\underline{\tilde{\phi}}: E\{\underline{\tilde{\phi}}^\dagger \underline{\tilde{\phi}}\} \leq tT_{\text{pay}}P} \frac{1}{T_{\text{pay}}} I(\underline{\tilde{y}}; \underline{\tilde{\phi}} | \hat{\mathbf{H}}), \quad (\text{nat/slot}) \quad (17)$$

where $I(\underline{\tilde{y}}; \underline{\tilde{\phi}} | \hat{\mathbf{H}})$ is the mutual information (Gallagher, 1968) conveyed by the MIMO uplink when $\hat{\mathbf{H}}$ is the (possibly imperfect) estimate of the uplink gains available at the transmit radio. Unfortunately, barring the limit cases of perfect channel state information (where $\hat{\mathbf{H}} = \mathbf{H}$) and no channel state information ($\hat{\mathbf{H}} = \mathbf{0}$), the probability density function (pdf) of the input signals $\underline{\tilde{\phi}}$ achieving the supremum in (17) is currently unknown (Baccarelli & Biagi, 2004; Paulraj et al., 2003; Baccarelli 2007). However, it is known that Gaussian distributed input signals reach the supremum in (17) both when $\hat{\mathbf{H}} = \mathbf{H}$, as well as for imperfect channels estimates (i.e., $\hat{\mathbf{H}} \neq \mathbf{H}$) when the length T_{pay} of the payload phase

(largely) exceeds the number of transmit antennas. Therefore, justified by the above considerations, in the sequel, we assume that the T_{pay} components $\{\underline{\phi}(n), T_{L1} + T_{L2} + 1 \leq n \leq T\}$ in (12) of the overall signal vector $\underline{\vec{\phi}}$ in (14) are uncorrelated proper complex Gaussian vectors, with correlation matrix \mathbf{R}_ϕ meeting (13). The corresponding throughput

$$\mathcal{R}(\hat{\mathbf{H}}) \triangleq \sup_{\text{Tra}[\mathbf{R}_\phi] \leq tP} \frac{1}{T_{pay}} I(\underline{\vec{y}}; \underline{\vec{\phi}} | \hat{\mathbf{H}}), \quad (\text{nat/slot}) \quad (18)$$

conveyed by MIMO uplink is the performance metric considered by the accessing cognitive radio Tx. About the analytic evaluation of $\mathcal{R}(\hat{\mathbf{H}})$ in (18), in (Baccarelli & Biagi, 2003; Biagi, 2006; Baccarelli et al., 2007) the following result is provided.

Proposition 1

Under the above reported assumptions about the considered access system, the $\hat{\mathbf{H}}$ -depending information- throughput $\mathcal{R}(\hat{\mathbf{H}})$ in (18) may be evaluated in closed form as in

$$\begin{aligned} I(\underline{\vec{y}}; \underline{\vec{\phi}} | \hat{\mathbf{H}}) = & T_{pay} \lg \det \left(\mathbf{I}_r + \frac{\beta}{t} \mathbf{K}_d^{-1/2} \hat{\mathbf{H}}^T \mathbf{R}_\phi \hat{\mathbf{H}}^* \mathbf{K}_d^{-1/2} + \beta \sigma_\varepsilon^2 P \mathbf{K}_d^{-1} \right) \\ & - \lg \det \left(\mathbf{I}_{rt} + \frac{\beta \sigma_\varepsilon^2 T_{pay}}{t} (\mathbf{K}_d^{-1})^* \otimes \mathbf{R}_\phi \right), \end{aligned} \quad (19)$$

when at least one of the following conditions is met:

1. both T_{pay} and t are large;
2. $\hat{\mathbf{H}}$ approaches \mathbf{H} ;
3. all SINRs γ_j in (11) vanish.

□

3.1 Optimized cognitive access policy

In order to compute the supremum in (18), we must proceed to carry out the power-constrained maximization of $\mathcal{R}(\hat{\mathbf{H}})$. For this purpose, let us indicate with

$$\mathbf{K}_d = \mathbf{U}_d \mathbf{\Lambda}_d \mathbf{U}_d^T, \quad (20)$$

the singular value decomposition (SVD) of the MAI spatial covariance matrix \mathbf{K}_d , where

$$\mathbf{\Lambda}_d \triangleq \text{diag}\{\mu_1, \dots, \mu_r\}, \quad (21)$$

is the corresponding $(r \times r)$ diagonal matrix of the magnitude-ordered singular values of \mathbf{K}_d . Thus, after introducing the $(t \times r)$ dummy matrix

$$\mathbf{A} \triangleq \hat{\mathbf{H}}^* \mathbf{K}_d^{-1/2} \mathbf{U}_d, \quad (22)$$

accounting for the combined effects of the imperfect channel estimate \hat{H} and the spatial MAI K_d , let us denote by

$$\mathbf{A} = \mathbf{U}_A \mathbf{D}_A \mathbf{V}_A^\dagger, \quad (23)$$

the corresponding SVD, where \mathbf{U}_A and \mathbf{V}_A are unitary matrices, while

$$\mathbf{D}_A = \begin{pmatrix} \text{diag}\{k_1, \dots, k_s\} & \mathbf{0}_{s \times r-s} \\ \mathbf{0}_{t-s \times s} & \mathbf{0}_{t-s \times r-s} \end{pmatrix}, \quad (24)$$

is the $(t \times r)$ diagonal matrix collecting the $s \triangleq \min\{r, t\}$ magnitude-ordered singular values $k_1 \geq k_2 \geq \dots \geq k_s > 0$ of the matrix \mathbf{A} . Finally, for future convenience, let us also introduce the following dummy positions:

$$\alpha_m \triangleq \frac{\mu_m k_m^2}{t(\mu_m + P\sigma_\varepsilon^2)}, \quad 1 \leq m \leq s; \quad \lambda_l \triangleq \frac{\sigma_\varepsilon^2 T_{\text{pay}}}{t\mu_l}, \quad 1 \leq l \leq r. \quad (25)$$

In this way, it can be proved (Baccarelli & Biagi, 2003; Biagi, 2006; Baccarelli et al., 2007) that an application of the Kuhn-Tucker conditions (Gallagher, 1968) leads to the following optimized access strategy for the cognitive Tx radio.

Proposition 2 (Optimized access strategy)

Let the assumptions reported in Proposition 1 be fulfilled. Therefore, for $m=s+1, \dots, t$ the powers $\{P^*(m)\}$ achieving the supremum in (18) vanish, while for $m=1, \dots, s$ they equate

$$P^*(m) = 0, \quad \text{when} \quad k_m^2 \leq \left(1 + \frac{\sigma_\varepsilon^2 P}{\mu_m}\right) \left(\frac{t}{\rho} + \sigma_\varepsilon^2 \text{Tra}\{\mathbf{K}_d^{-1}\}\right), \quad (26)$$

$$P^*(m) = \frac{1}{2\lambda_{\min}} \left\{ \lambda_{\min} L - 1 + \sqrt{(\lambda_{\min} L)^2 + 4\lambda_{\min} \left(\rho - \frac{1}{\alpha_m} - \frac{r\rho\lambda_m}{\alpha_m T_{\text{pay}}} \right)} \right\}, \quad (27)$$

when $k_m^2 > \left(1 + \frac{\sigma_\varepsilon^2 P}{\mu_m}\right) \left(\frac{t}{\rho} + \sigma_\varepsilon^2 \text{Tra}\{\mathbf{K}_d^{-1}\}\right)$

where $\lambda_{\min} \triangleq \min\{\lambda_l, l=1, \dots, r\}$ and $L \triangleq \left(1 - (r/T_{\text{pay}})\right)\rho - (1/\alpha_m)$. Furthermore, the non-negative scalar parameter ρ in (26), (27) is set to meet the following power-constraint:

$$\sum_{m \in \mathcal{I}(\rho)} P^*(m) \equiv P, \quad (28)$$

where

$$\mathcal{I}(\rho) \triangleq \left\{ m = 1, \dots, s : k_m^2 > \left(1 + \frac{\sigma_\varepsilon^2 P}{\mu_m} \right) \left(\frac{t}{\rho} + \sigma_\varepsilon^2 \text{Tra} \{ \mathbf{K}_d^{-1} \} \right) \right\}, \quad (29)$$

is the (ρ -dependent) set of m -indexes fulfilling the inequality in (27). Finally, the corresponding optimized spatial correlation matrix $\mathbf{R}_\phi(\text{opt})$ of the radiated signals is aligned along the right eigenvectors of the matrix \mathbf{A} in (22) as in

$$\mathbf{R}_\phi(\text{opt}) = \mathbf{U}_A \text{diag} \{ P^*(1), \dots, P^*(s), \mathbf{0}_{t-s} \} \mathbf{U}_A^T, \quad (30)$$

so that for the resulting conveyed throughput $\mathcal{R}(\hat{\mathbf{H}})$ we have

$$\mathcal{R}(\hat{\mathbf{H}}) = \sum_{m=1}^r \lg \left(1 + \frac{\sigma_\varepsilon^2 P^*(m)}{\mu_m} \right) + \sum_{m=1}^s \left(\lg (1 + \alpha_m P^*(m)) \right) \quad (\text{nat/slot}). \quad \square \quad (30.1)$$

3.2 MAI-learning and MAI-mitigation at the AP

Before proceeding to detect the transmitted packet, the AP may attempt to estimate the MAI component $\underline{d}(n)$ affecting the received signal $\underline{y}(n)$ in (12), so as to subtract the computed MAI estimate $\hat{\underline{d}}(n)$ from the received signal $\underline{y}(n)$. Since both \mathbf{K}_d and $\hat{\mathbf{H}}$ are available at the AP, this last is also aware of $\mathbf{R}_\phi(\text{opt})$ (equation (30)), so that it may exploit both $\hat{\mathbf{H}}$ and $\mathbf{R}_\phi(\text{opt})$ to improve the MAI estimate's accuracy. Specifically, being $\phi(n)$ and $\underline{d}(n)$ Gaussian distributed, the MMSE estimate $\hat{\underline{d}}(n) \triangleq E\{\underline{d}(n) | \underline{y}(n)\}$ of the MAI is linear with respect to the observation $\underline{y}(n)$ (Poor, 1994), so that we may write

$$\hat{\underline{d}}(n) = \mathbf{F} \underline{y}(n). \quad (31)$$

In turns, the $(r \times r)$ matrix \mathbf{F} in (31) may be computed via an application of the (usual) Orthogonal Principle (Poor, 1994), that allows us to write

$$E\{(\hat{\underline{d}}(n) - \underline{d}(n))(\underline{y}(n))^T | \hat{\mathbf{H}}, \mathbf{R}_\phi(\text{opt})\} = \mathbf{0}_{r \times r}, \quad (32)$$

where the conditioning in (32) accounts for the availability of $\hat{\mathbf{H}}$ and $\mathbf{R}_\phi(\text{opt})$ at the AP side (e.g., the AP is cognitive). Hence, by developing the expectations in (32), after some (tedious) algebra, we arrive at the following final expression for the matrix \mathbf{F} in (31):

$$\mathbf{F} = \left\{ \frac{\beta}{t} \left[\hat{\mathbf{H}}^T \mathbf{R}_\phi(\text{opt}) \hat{\mathbf{H}}^* + P t \sigma_\varepsilon^2 \mathbf{I}_r \right] \mathbf{K}_d^{-1} + \mathbf{I}_r \right\}^{-1}. \quad (33)$$

The MSE performance of the estimator in (31) is dictated by the corresponding error covariance matrix $K_{de} \triangleq E\{(\hat{\underline{d}}(n) - \underline{d}(n))(\hat{\underline{d}}(n) - \underline{d}(n))^{\dagger} | \hat{\underline{H}}, R_{\phi}(opt)\}$ that equates (equations (31), (33))

$$K_{de} = [I_r - F]K_d. \quad (34)$$

Roughly speaking, equation (34) measures the performance improvement arising from the exploitation of the cognitive capability of the AP node. In particular, equation (33) points out that F vanishes for vanishing K_d , while F approaches I_r for large K_d . As a consequence, on the basis of equation (34), we conclude that actual effectiveness of the MAI estimation/subtraction procedure implemented by the AP tends to improve in the presence of strong MAI.

4. Some Game Theory essentials

In order to model the dynamic behaviour of the uplink-state of the access system of Fig. 1(a), we resort to the formal tool of the Game Theory. We shortly recall that a non-cooperative and strategic game $G \triangleq \langle \mathbb{N}, A, \{u_g\} \rangle$ has three components (MacKenzie & Wicker, 2001; Fudenberg & Tirole, 1991): a finite set $\mathbb{N} \triangleq \{1, 2, \dots, n^*\}$ of players, a set $A_g, g \in \mathbb{N}$, of admissible actions for the g -th player and a set of utility functions. Specifically, after denoting as $A \triangleq A_1 \times A_2 \times \dots \times A_{n^*}$ the space of action profiles, let us indicate as $u_g : A \rightarrow \mathbb{R}$ the utility function of the g -th player. Therefore, after indicating by $\underline{a} \in A$ an action profile, by $a_g \in A_g$ the action of g -th player in \underline{a} and by \underline{a}_{-g} the actions in \underline{a} of the other $(n^* - 1)$ players, we can say that $u_g(\underline{a}) \equiv u_g(a_g, \underline{a}_{-g})$ maps² each action profile \underline{a} into a real number. In particular, in a strategic non-cooperative game each player chooses a suitable action a_g^* from his action set A_g to maximize its own utility function, according to the following game rule:

$$a_g^* \equiv \max_{a_g \in A_g} u_g(a_g, \underline{a}_{-g}). \quad (35)$$

Therefore, since there is no cooperation among the players, it is important to ensure the dynamic stability of the overall game. A concept which relates to this issue is the so-called Nash Equilibrium (NE). Simply stated, a NE is an action profile \underline{a}^* at which no player may gain by unilaterally deviating from. So, a NE is a stable operating point of the game, because

² The notation $u_g(a_g, \underline{a}_{-g})$ emphasizes that the g -th player controls only own action a_g , but his achieved utility depends also on the actions \underline{a}_{-g} taken by all remaining players (MacKenzie & Wicker, 2001; Fudenberg & Tirole, 1991).

no player can obtain any profit from a change in his strategy. Formally stated, a NE is an action profile \underline{a}^* such that for all $a_g \in A_g$ the following inequality is met:

$$u_g(a_g^*, \underline{a}_{-g}^*) \geq u_g(a_g, \underline{a}_{-g}^*), \quad \forall a_g \in A_g, \quad \forall g \in \mathbb{N}. \quad (36)$$

5. The proposed cognitive access game

Let us focus now on the uplink in Fig. 1(a) of a WLAN composed by n^* mutually interfering multi-antenna accessing radios. The ultimate task of the g -th radio terminal is to maximize the information throughput $\mathcal{R}(g)$ (nat/slot), sustained by the corresponding uplink $T_g \rightarrow AP$ via suitable power-allocation and shaping of the transmitted signals and interference cancellation at the AP. Since the signals radiated by g -th radio induce MAI at the AP side and we assume that the radios do not exchange information (the accessing terminals do not cooperate), we may model the interaction among the accessing cognitive radios as a non-cooperative strategic game. Specifically, in the considered access scenario, the players' set \mathbb{N} is composed of n^* accessing radios, while the set of actions A_g available to the g -th player is the set of all covariance matrices $\mathbf{R}_\phi^{(g)}$ meeting the power constraint (2), so we can pose

$$A_g \equiv \left\{ \mathbf{R}_\phi^{(g)} : 0 \leq \text{Tra}[\mathbf{R}_\phi^{(g)}] \leq t_g P^{(g)} \right\} \quad g = 1, \dots, n^*, \quad (37)$$

where $P^{(g)}$ (Watt) is the power available at the g -th radio and t_g is the number of transmit antennas equipping the g -th radio. This means that the generic action a_g of T_g consists in the transmission of a Gaussian distributed payload sequence with covariance matrix $\mathbf{R}_\phi^{(g)}$. Furthermore, the utility function $u_g(\cdot)$ for the g -th access link is the corresponding conveyed rate, so that we can write (equation (9))

$$\begin{aligned} u_g(\underline{a}) &\triangleq u_g(\mathbf{R}_\phi^{(1)}, \dots, \mathbf{R}_\phi^{(g)}, \dots, \mathbf{R}_\phi^{(n^*)}) \equiv \frac{1}{T_{pay}} I(\underline{\tilde{y}}^{(g)}; \underline{\tilde{\phi}}^{(g)} | \hat{\mathbf{H}}_g) \\ &\equiv \lg \det \left(\mathbf{I}_r + \frac{\beta_g}{t_g} (\mathbf{K}_d^{(g)})^{-1/2} \hat{\mathbf{H}}_g^T \mathbf{R}_\phi^{(g)} \hat{\mathbf{H}}_g^* (\mathbf{K}_d^{(g)})^{-1/2} + \beta_g \sigma_\varepsilon^2(g) P^{(g)} (\mathbf{K}_d^{(g)})^{-1} \right) \\ &\quad - \frac{1}{T_{pay}} \lg \det \left(\mathbf{I}_{rt_g} + \frac{\beta_g \sigma_\varepsilon^2(g) T_{pay}}{t_g} \left((\mathbf{K}_d^{(g)})^{-1} \right)^* \otimes \mathbf{R}_\phi^{(g)} \right), \end{aligned} \quad (38)$$

where the g -th MAI covariance matrix $K_d^{(g)}$ depends on the spatial covariance matrices $\{R_\phi^{(i)}, i \neq g\}$ of the signals radiated by all other accessing radios (Fig. 1(b))³. About the rule of the game, each player (i.e., accessing cognitive radio T_g) chooses the action $R_\phi^{(g)*}$ which maximize the throughput conveyed by its own access link, so we can write

$$R_\phi^{(g)*} \equiv \arg \max_{R_\phi^{(g)} \in A_g} \left\{ \frac{1}{T_{pay}} I(\bar{y}^{(g)}; \bar{\phi}^{(g)} | \hat{H}_g) \right\}, \quad g = 1, \dots, n^*. \quad (39)$$

5.1 Competitive optimal SDMA

We pass now to detail the algorithm for the competitively optimal access under ‘contracted-QoS’ and best-effort policies when the AP of Fig. 1(a) performs MAI estimation/subtraction. Before proceeding, we point out that the concept of ‘contracted-QoS’ we go to introduce relies on multiple QoS classes defined in terms of requested, or desired, access throughput. Therefore, the resulting access algorithm we report in Table 1 attempts to achieve the target throughput $T\mathcal{R}_A^{(Z)}$ desired by the g -th radio; and if this throughput is not achievable due to the MAI induced by the other accessing terminals, the algorithm tries to achieve the next lower QoS-class $T\mathcal{R}_A^{(Z-1)}$.

Furthermore, from the outset it also follows that the best-effort policy is an instance of the ‘contracted-QoS’ one, where the number of allowed QoS classes approach infinity. The algorithm for achieving the competitively maximal access throughput over the uplink is detailed in Table 1. It must be iteratively run by all accessing radios of Fig. 1(a). $T\mathcal{R}_A^{(Z)}$ (nat/slot) in Table 1 indicates the target throughput defining the Z -th QoS class.

0	Set the target throughput $T\mathcal{R}_A^{(Z)}$ of the Z -th QoS class
1	Initialize $R_\phi^{(g)}$ (new) := $R_\phi^{(g)}$ (old) = $0_{t_g \times t_g}$
2	$fl(g) = 1$
3	$\mathcal{R}(g) = 0$
4	$a^{(g)} \triangleq (\bar{P}T_{tr}/r_g) Tra \left[(K_d^{(g)})^{-1} \right]$
5	$\sigma_\varepsilon^2(g) \triangleq (1 + a^{(g)}/t_g)^{-1}$
6	Compute and sort the r eigenvalues of $K_d^{(g)}$
7	Compute the SVD of $\hat{H}_g^* K_d^{(g)-1} \hat{H}_g^T$
8	Sort the $s \triangleq \min(r, t)$ eigenvalues $\{k_1^{(g)2}, \dots, k_s^{(g)2}\}$ of $K_d^{(g)}$
9	$\alpha_m^{(g)} \triangleq \mu_m^{(g)} k_m^{(g)2} / t_g \left(\mu_m^{(g)} + P^{(g)} \sigma_\varepsilon^2(g) \right)$
10	$\beta_l^{(g)} \triangleq \sigma_\varepsilon^2(g) T_{pay} / \mu_l^{(g)} t_g$

³ In the sequel, we adopt the index g for indicating the system parameters of the g -th uplink $T_g \rightarrow AP$ (Fig. 1(a)).

```

11       $\mu_{min}^{(g)} \triangleq \min_{1 \leq l \leq r} \left\{ \mu_m^{(g)} \right\}; \rho_{max}^{(g)} \triangleq \frac{\sigma_{\varepsilon}^2(g) T_{pay}}{\mu_{min}^{(g)} t_g}$ 
12      If  $k_m^{(g)2} \geq \left( \mu_m^{(g)} + p^{(g)} \sigma_{\varepsilon}^2(g) \right) \frac{\sigma_{\varepsilon}^2(g) \sqrt{r T_{pay}}}{\mu_{min}^{(g)} \mu_m^{(g)}}$  for all  $m$  and  $fl(g)=1$ 
{
13      Set  $\rho^{(g)} := 0$  and  $\rho^{(g)} := 0$   $\mathcal{J}(\rho^{(g)}) := 0$ 
14      Set the step size  $\Delta$ 
15      While  $\sum_{m \in \mathcal{J}(\rho^{(g)})} P^{*(g)}(m) < P$  do
{
16      Update  $\rho^{(g)} = \rho^{(g)} + \Delta$ 
17      Update the set  $\mathcal{J}(\rho^{(g)})$  via equation (29)
18      Compute the powers and the covariance matrix via equation (26), (27), (30)
19      Set  $\Psi^{(g)} := \mathbf{R}_{\phi}^{(g)}(new) - \mathbf{R}_{\phi}^{(g)}(old)$ 
20      If  $\left( \left\| \Psi_E^{(g)} \right\|_E^2 \leq 0.05 \left\| \mathbf{R}_{\phi}^{(g)}(old) \right\|_E^2 \right)$ 
21      then  $fl(g)=0$ , else  $fl(g)=1$ ;
22       $\mathbf{R}_{\phi}^{(g)}(old) := \mathbf{R}_{\phi}^{(g)}(new)$ 
}
23      Evaluate  $\mathcal{R}(g)$  via (30.1) for the  $g$ -th link
24      If  $\mathcal{R}(g) = T \mathcal{R}_A^{(Z)}$  stop; else
25      If  $\mathcal{R}(g) = T \mathcal{R}_A^{(Z)}$  reduce the radiate power  $P^{(g)}$  and go to Step 1; else
26      If  $\mathcal{R}(g) > T \mathcal{R}_A^{(Z)}$  lower the target class to (Z-1) and go to Step 1.
}

```

Table 1. Pseudocode implementing the competitively optimal cognitive access on the g -th uplink under the 'contracted-QoS' policy

5.2 Asynchronous implementation of the access game and Nash Equilibria

After assuming that the access algorithm of Table 1 is iteratively run (in a non-cooperative and possibly asynchronous way) by all accessing radios of Fig. 1(a), let be $V_g \triangleq \{t_{g1}, t_{g2}, \dots\}$ the set of times at which g -th radio executes this algorithm. Thus, after indicating by $V \triangleq \{\tau_1, \tau_2, \dots\}$ the resulting overall set of update times $V_1 \cup V_2 \cup \dots \cup V_{n^*}$ sorted in the increasing order ($\tau_i \leq \tau_{i+1}$), the asynchronous and distributed implementation of the considered access game works according to the pseudocode of Table 2.

Hence, key-questions about the access game of Table 2 regard the existence, uniqueness and achievability of the corresponding NE. The following *Proposition 3* (Biagi, 2006) gives insight about these questions.

```

For all k such that  $\tau_k \in V$ 
{
For all terminals  $g \in \mathbb{N}$  such that  $\tau_k \in V_g$ 
{
Evaluate the MAI matrix  $K_d^{(g)}$ 
Run the algorithm of Table 1 so
to compute  $[\underline{\phi}^{(g)}]$  and  $[R_{\phi}^{(g)}]$ 
radiate the signal vector  $[\underline{\phi}^{(g)}]$ 
}
}

```

Table 2. Pseudocode implementing the proposed access game

Proposition 3

By referring to the access game of Table 2, let us assume that the following conditions are met:

$$k_m^{(g)^2} > \left(1 + \frac{\sigma_\varepsilon(g)^2 P^{(g)}}{\mu_m(g)}\right) \left(\frac{t_g}{\rho} + \sigma_\varepsilon(g)^2 \text{Tra}[K_d^{(g)-1}]\right) \quad (40)$$

$$r \geq t_g, \quad 1 \leq g \leq n^* \quad (41)$$

$$T_{\text{pay}} \gg T_g > 1 \text{ and / or } \sigma_\varepsilon(g)^2 \rightarrow 0, \quad 1 \leq g \leq n^*. \quad (42)$$

Thus, the NE of the access game of Table 2 exists, is unique and it may be reached by moving from any starting point.

6. Cognitive MIMO access performance

Since WLANs are characterized by topology-depending time-varying MAI, in principle, an effective SDMA protocol should be able to adaptively exploit (in a combined way) the above mentioned flexibility characteristics of the MIMO physical layer by operating in a scalable and asynchronous way. Currently, Carrier Sense Multiple Access with Collision Avoidance (CSMA/CA) is 'de-facto' the MAC protocol considered for WLANs. Interestingly enough, a simple extension of CSMA/CA for MIMO links can be designed to provide an $s = \min(t, r)$ -fold improvement in throughput performance compared to a single-input single-output (SISO) network. We refer to this simple extension as CSMA/CA(s). Essentially, CSMA/CA(s) operates in the same fashion as the conventional CSMA/CA, except that all transmissions are performed using s independent parallel streams, so as to attain a spatial multiplexing gain. Such a protocol is still collision-free, and, when compared to default single-antenna CSMA/CA, it is able to achieve s times the throughput performance than the latter. Thus, while this s -fold improvement guaranteed by the collision-free CSMA/CA(s) is, indeed, quite appealing, the key question we proceed to tackle is: Is it possible for a more 'smart' SDMA scheme to attain a better throughput performance by working in a scalable and asynchronous way? We anticipate that the main conclusion we arrive at, is, indeed yes. Roughly speaking, the key-rationale behind this conclusion is that CSMA/CA(s) is still a

collision-free MAC scheme, so that it is not able to fully exploit the advantages arising from the above mentioned flexible MAI-mitigation capability of the MIMO physical layer.

To corroborate this claim, we simulated a Rayleigh-flat faded WLAN composed of $n^* = 2$ accessing radios located at a same distance of $D_1 = D_2 = 100$ (mt) from the AP. The fading phenomena impairing the uplinks $T_1 \rightarrow AP$ and $T_2 \rightarrow AP$ are equidistributed and mutually independent. No obstacles are assumed between the accessing radios and the AP, so that MAI and signal average power levels measured only depend on the path-loss. All the reported numerical results refer to a path-loss exponent of 2.5, while the average received signal-to-noise ratio (SNR) is 20 dB. Furthermore, unless otherwise stated, the MMSE estimates $\{\hat{h}_{ji}^{(g)}, g = 1, 2\}$ of the uplink gains available at the radios are assumed exact (i.e., error free).

6.1 The achievable throughput regions

In this operating conditions, the (two-dimensional) set of accessing rates sustainable by the AN may be (formally) described by resorting to the concept of achievable rate-region (Baccarelli et al., 2005). In a nutshell, given a statistical description of the uplinks $T_1 \rightarrow AP, T_2 \rightarrow AP$, and under an assigned set of constraints on the available radio resources (e.g., available power, bandwidth, noise level, and so on), the corresponding achievable rate region of the access network is the closure of all 2-ple $(\mathcal{R}_1, \mathcal{R}_2)$ of the access rates that may be simultaneously sustained by the network.

Unfortunately, apart from some partial contributions, no closed-form analytical formulas are available yet for the evaluation of the rate-region of MAI-impaired access networks (Baccarelli et al., 2005). Forced by this consideration, we resort to numerical tests and Fig. 2 reports the rate-regions we have numerically obtained for some different access strategies. The $n^* = 2$ radios of the simulated access network of Fig. 2 are equipped with $t_1 = t_2 = 4$ transmit antennas, while $r = 4$ receive antennas are available at the AP. The innermost \mathcal{A} -labelled region of Fig. 2 reports the sustainable access rates when the power available at the radios is evenly split over the transmit antennas (i.e. $\mathbf{R}_\phi^{(1)} = \mathbf{R}_\phi^{(2)} = \frac{P}{4} \mathbf{I}_4$ in equation (39)) and,

in addition, no channel estimate are available for MAI mitigation ($\hat{\mathbf{H}} = \mathbf{0}$ in equation (33), so that the AP node is no cognitive). In this case, when both the radios attempt to access to the AP, the resulting maximal throughput is quite low and it is limited up to $\mathcal{R}_1 = \mathcal{R}_2 = 11$ (bit/slot). However, when the AP performs reliable MAI estimation and subtraction (i.e. $\hat{\mathbf{H}} \equiv \mathbf{H}$ in equation (33) and thus the AP node is perfectly cognitive), we obtain the (larger) rate-region \mathcal{B} of Fig. 2, that covers the above \mathcal{A} -region and allows radios to simultaneously access at a maximal throughput of $\mathcal{R}_1 = \mathcal{R}_2 = 16.5$ (bit/slot).

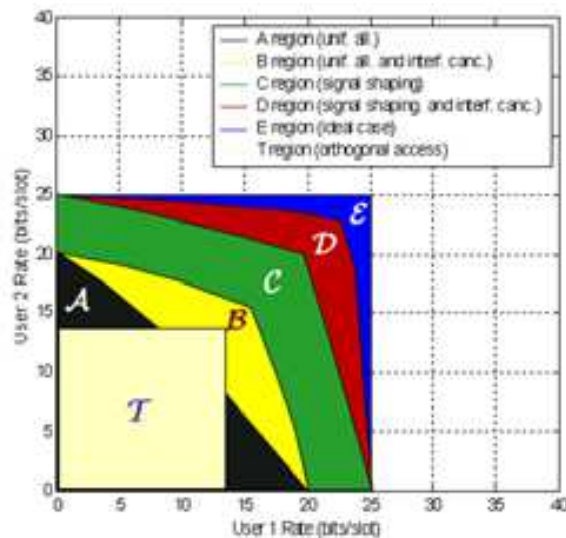


Fig. 2. Rate regions for some different accessing policies and systems setting

When optimized power-allocation and signal-shaping are also performed at the radios (that is, $\mathbf{R}_\phi^{(g)}$ are computed as in equation (39)) but no reliable MAI-mitigation is performed by the AP, we obtain the rate-region \mathcal{C} of Fig. 2 that allows radios to simultaneously access at a (maximal) throughput of $\mathcal{R}_1 = \mathcal{R}_2 = 21$ (bit/slot). A comparison of \mathcal{D} and \mathcal{E} regions of Fig. 2 gives insight on the ultimate effectiveness of the competitive SDMA game played by the cognitive radios and the MAI mitigation performed by the cognitive AP. Specifically, the \mathcal{D} region of Fig. 2 collects the 2-ple $(\mathcal{R}_1, \mathcal{R}_2)$ of achievable access rates when both the competitive SDMA game of Table 2 is carried out by the radios and a reliable MAI estimation/subtraction is performed by the AP. In this case, the maximal access throughput sustained by the AN approaches $\mathcal{R}_1 = \mathcal{R}_2 = 23.5$ (bit/slot). This value differs, indeed, less than 6% from the ultimate one of $\mathcal{R}_1 = \mathcal{R}_2 = 25$ (bit/slot) bounding the corresponding \mathcal{E} region. This last refers to the ideal case when MAI-cancellation is perfect (i.e. $\hat{\mathbf{d}}(n) \equiv \mathbf{d}(n)$ in equation (31)) and both radios are allowed to transmit over the whole working-time of the system.

About the degrading effects induced by possibly imperfect MIMO uplink estimates, these last have been investigated in depth, for example, in (Baccarelli & Biagi, 2003; Baccarelli & Biagi, 2004). So, in this context we limit to remark that the \mathcal{A} -region of Fig. 2 represents the sustainable access rates when both radios and AP are fully unaware about actual values of the MIMO uplink gains (in other words, they are not cognitive and $\hat{\mathbf{H}}^{(1)} = \hat{\mathbf{H}}^{(2)} = 0$), while the corresponding \mathcal{D} -region captures the achievable access rates when both radios and AP are equipped with perfect MIMO uplink estimates (i.e. $\hat{\mathbf{H}}^{(1)} = \mathbf{H}^{(1)}$ and $\hat{\mathbf{H}}^{(2)} = \mathbf{H}^{(2)}$). A direct comparison of these regions leads to the conclusion that the penalty in the access throughput arising from full unawareness about MIMO uplink-gains may be, indeed, no negligible and of the order of 5–6 (bit/slot) per accessing radio. Obviously, this conclusion is somewhat mitigated by considering that long throughput-consuming learning phases may be required in order to acquire reliable uplink estimates (Section 3.2). The interested reader

may refer to the works in (Baccarelli & Biagi, 2003; Baccarelli & Biagi, 2004; Baccarelli et al., 2007) and references therein for a detailed description of the optimal estimation accuracy - vs. - throughput trade off.

6.2 Cognitive SDMA Game-vs-CSMA/CA(s): a throughput comparison

The effectiveness of the proposed competitive SDMA policy for cognitive ANs may be also appreciated by comparing the above mentioned \mathcal{D} -region against the one of Fig. 2. Specifically, this \mathcal{T} -region of Fig. 2 reports the 2-ple $(\mathcal{R}_1, \mathcal{R}_2)$ of achievable access rates when the access policy followed by the (no cognitive) multi-antenna radios is the CSMA/CA(s). In this regard, we explicitly stress that, to guarantee both collision-free and fair access, in the carried out numerical tests the CSMA/CA(s) policy we implemented schedules a single uplink at a time, and transmits over the scheduled uplink at the maximum allowed power P and over a $1/n^* = 1/2$ -fraction of the overall system working time. Furthermore, the throughput loss due to the (possible) exchange of RTS/CTS packets is not accounted for. Thus, being the implemented CSMA/CA(s) scheme collision-free (that is, fully MAI-free), the corresponding \mathcal{T} -region of Fig. 2 is the largest attainable by the CSMA/CA(s) policy. Now, an examination of Fig. 2 leads to the conclusion that the access region achieved by the CSMA/CA(s) policy is strictly included in the \mathcal{D} -region obtained by the proposed competitive cognitive-based SDMA policy, at least in the considered MAI-limited access scenario. Since the implemented CSMA/CA(s) strategy is, indeed, an example of multi-antenna orthogonal access policy, we conclude that the rate-region of any multi-antenna orthogonal access strategy (such as TDMA, FDMA, CDMA) overlaps the \mathcal{T} -region of Fig. 2. This supports the superiority of the proposed competitively optimal cognitive access strategy over the orthogonal no-cognitive ones, at least when the spatial-dimension offered by the AN may be efficiently exploited to perform both signal-beam forming at the accessing (cognitive) radios and MAI-mitigation at the (cognitive) AP.

6.3 Cognitive access capacity

The following Figs 3, 4 and 5 give insight into the performance of the proposed cognitive SDMA game with MAI-mitigation in terms of access capacity (i.e., in terms of maximum number of radios capable to simultaneously access the network at a common target throughput). The plots of Fig. 3 report the (numerically evaluated) system capacity at access throughput of 10, 15, 20 (bit/slot) when all radios are equipped with $t=4$ transmit antennas, while the AP performs MAI-mitigation via a number of receive antennas ranging from one to eight. An examination of these plots leads to two main conclusions. The first (quite obvious) one is that the access capacity decreases for increasing values of the target access throughput (the target QoS-level) demanded by the radios. The second (less trivial) one is that, at any target QoS level, the slope of the capacity curves of Fig. 3 grows for increasing r up to $r=t=4$, and then it starves for $r>t=4$. Due to the iterative nature of the proposed access strategy of Table 2, we are not able to give formal (e.g., analytical) support to this behaviour. However, roughly speaking, it may be understood by noting that, under mild assumptions, the Shannon capacity (in bit/slot) of a point-to-point flat-faded MIMO channel scales as the $\min(r, t)$ (Paulraj et al., 2003), so that no slope increment in the capacity curves is expected when $r>t$. However, by increasing r beyond t , MAI mitigation

capability of the AP still grows, so that the capacity curves of Fig. 3 increases (at a nearly constant rate) for growing values of r .

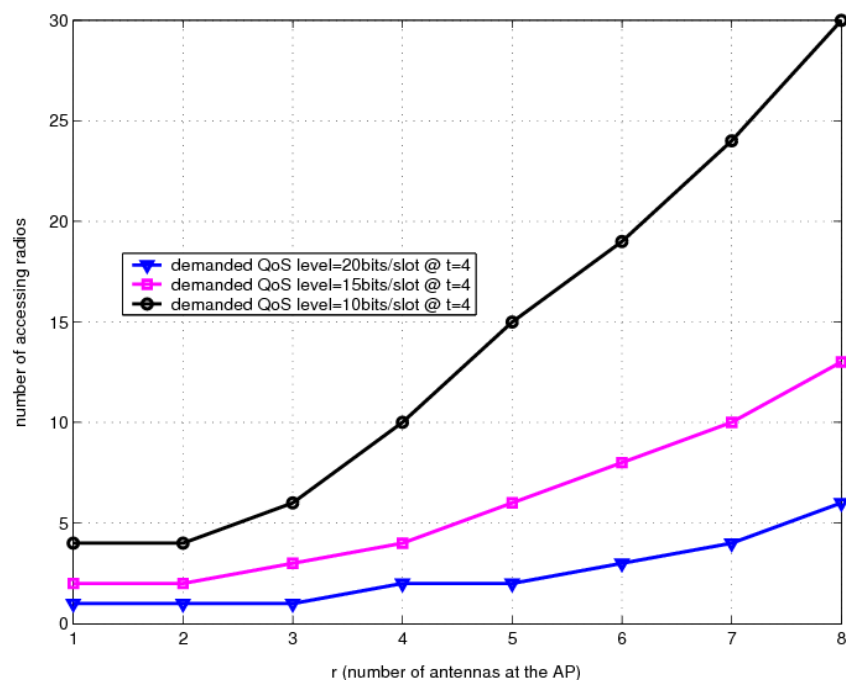


Fig. 3. Number of radios accessing the net under the guaranteed QoS policy for various r values

Similar conclusions may be drawn after an examination of the plots of Fig. 4, that capture the effects induced by the number t of transmit antennas equipping each accessing radio. Interestingly, a comparison of the curves of Fig. 3 and 4 shows that, at any target access throughput, the capacity of the access system with $t = m$ transmit antennas and $r = n$ receive ones outperforms the corresponding capacity of the 'dual' access system with $r = m$ and $t = n$. This behaviour supports the conclusion that, at least in the considered operating scenarios, the increment in the access capacity arising from more accurate transmit beam forming outperforms the corresponding capacity improvement due to more reliable MAI-mitigation. Finally, Fig. 5 reports the system capacity under the above mentioned 'contracted-QoS' access policy (Table 1), when the radios accept access throughput within 10% of the desired one. A comparison of the plots of Fig. 5 corroborates the conclusion that the 'QoS-contracted' access policy may be valuable in terms of system capacity, especially when the MAI-mitigation capability of the AP is limited (e.g., when the number r of the receive antennas is less than that of the transmit ones).

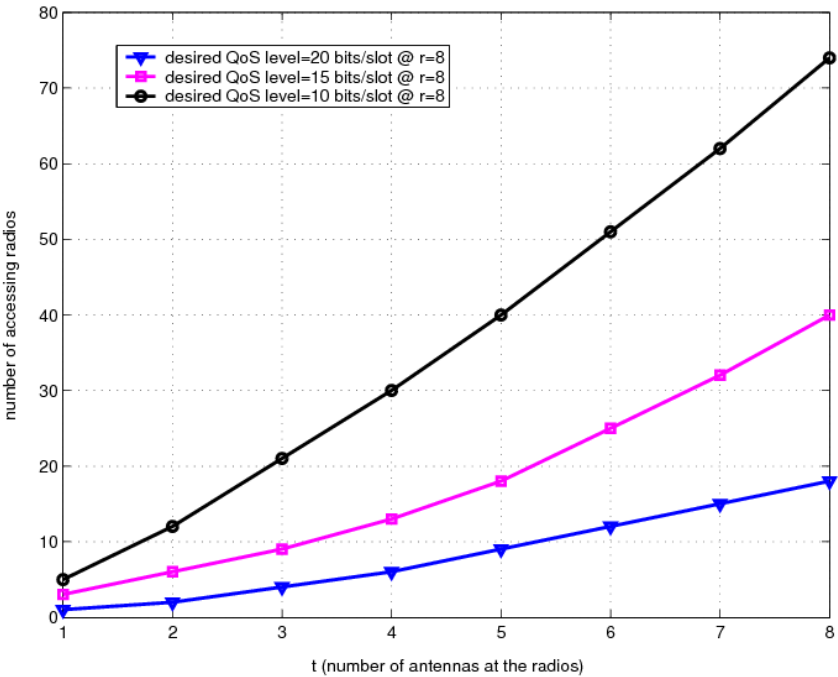


Fig. 4. Number of radios accessing the net under the guaranteed QoS policy for various t values

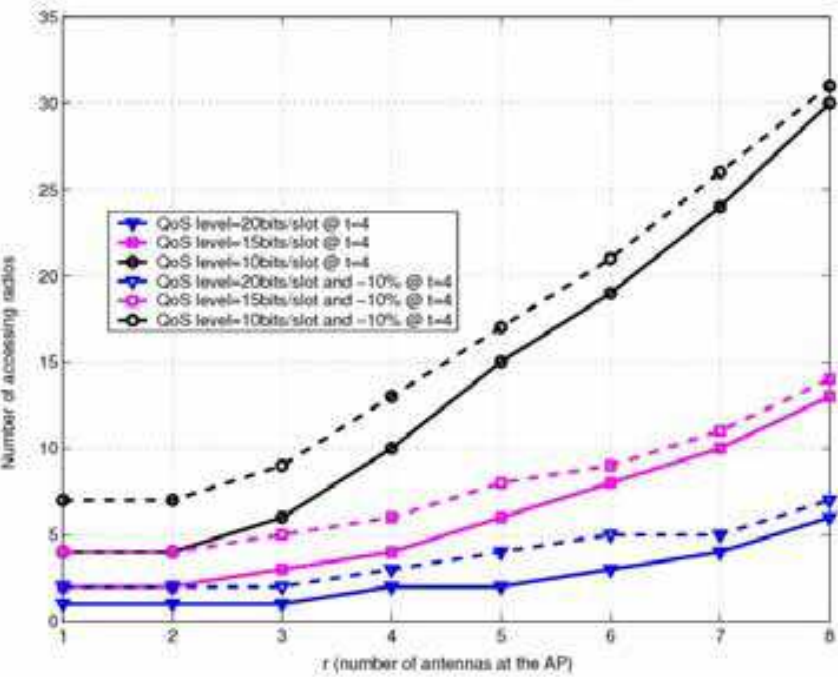


Fig. 5. Number of radios accessing the net under the 'contracted-QoS' policy for various r values

6.4 Self-convergence of the cognitive SDMA Game toward the nearest sustainable operating point

In actual application scenarios, the accessing radios are not aware in advance about the sustainable access regions of Fig. 2, neither these last may be analytically evaluated in closed-form (Baccarelli et al., 2005). Therefore, a key-question concerns the self-convergence of the operating point of the SDMA cognitive game of Table 2, when the initial access throughput $(\mathcal{R}_1^{(0)}, \mathcal{R}_2^{(0)})$ demanded by the radios falls out of the corresponding access region of Fig. 6. It can be proved (Biagi, 2006, Appendix 3) that, under the best-effort policy, the operating point of the SDMA game of Table 2 is able to self-move from $(\mathcal{R}_1^{(0)}, \mathcal{R}_2^{(0)})$ and to converge to the boundary point of the underlying access region at the minimum Euclidean distance from that starting point (see the dotted arrow of Fig. 6). Likewise, under the 'contracted-QoS' policy, the operating point self-moves from $(\mathcal{R}_1^{(0)}, \mathcal{R}_2^{(0)})$ to the point of the QoS grid at the minimum Euclidean distance (see the dashed grid of Fig. 6).

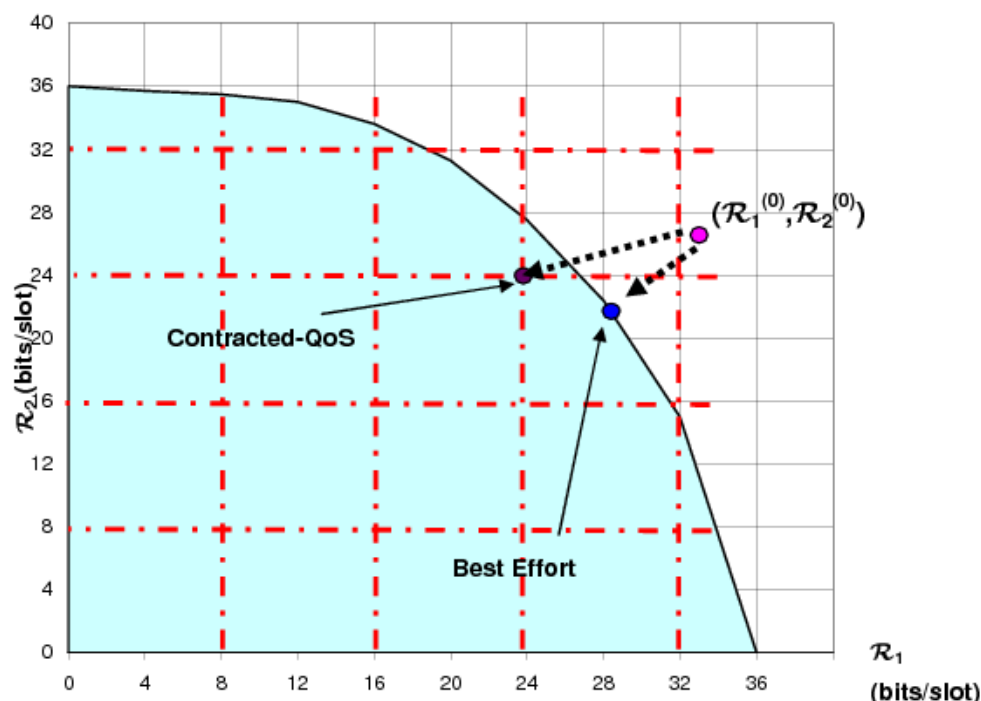


Fig. 6. Access region of the proposed cognitive SDMA game of Table 2 with MAI-mitigation ($t_1=t_2=4$ and $r=4$)

6.5 Mismatches in the estimation of the MAI covariance matrix

To test the sensitivity of the proposed cognitive SDMA game on errors possibly affecting the estimated MAI covariance matrices $\hat{K}_d^{(g)}$, $g=1, \dots, n^*$, we have perturbed actual matrices $K_d^{(g)}$, $g=1, \dots, n^*$, via randomly-generated $(r \times r)$ matrices $G^{(g)}$, $g=1, \dots, n^*$, which are composed by zero-mean proper complex unit-variance uncorrelated Gaussian elements. In doing so, we generated

$$\hat{K}_d^{(g)} = K_d^{(g)} + \sqrt{\frac{\|K_d^{(g)}\|_E^2}{r^2}} \sqrt{\delta} G^{(g)}, \quad g = 1, \dots, n^*, \quad (43)$$

where $\delta \triangleq E\left\{\|K_d^{(g)} - \hat{K}_d^{(g)}\|_E^2\right\} / \|K_d^{(g)}\|_E^2$ was set according to the desired average squared estimation errors affecting $\hat{K}_d^{(g)}$. Thus, after replacing the actual covariance matrices $K_d^{(g)}$ with the corresponding perturbed ones $\hat{K}_d^{(g)}$, we have played once again the SDMA Game of Table 2 for the same access scenario previously described in Section 6.1. The resulting access region (labelled as \mathcal{D}^*) is reported in Fig. 7, together with the corresponding \mathcal{D} -region previously drawn in Fig. 2 for the case of perfect MAI covariance-matrix estimates. An examination of the regions of Fig. 7 points out that the resulting access throughput-loss is limited up to 4%, even for δ values as high as 0.05.

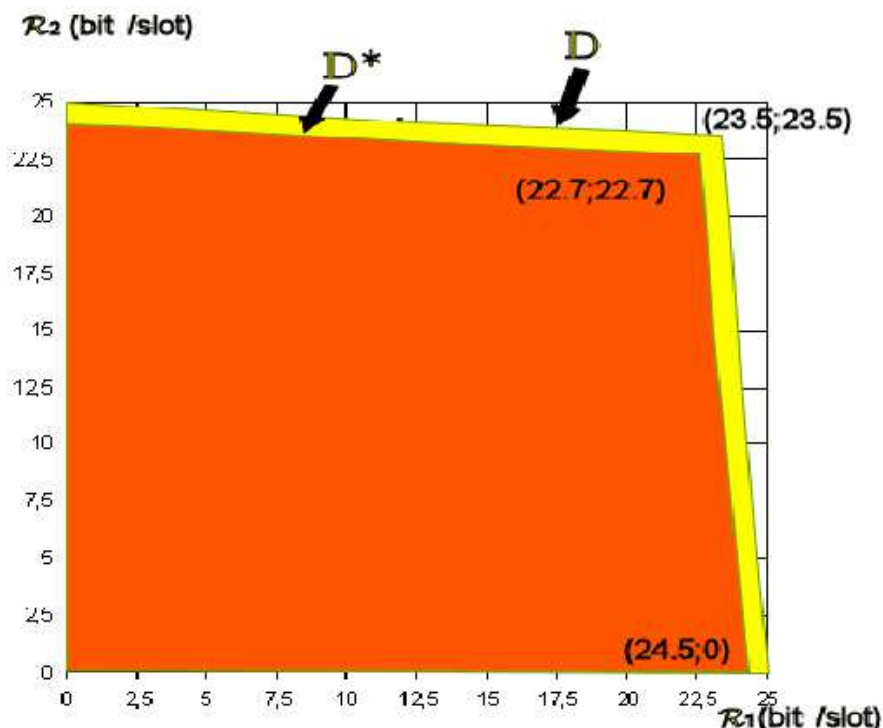


Fig. 7. Access regions for perfectly estimated MAI-covariance matrices (\mathcal{D}) and with estimation errors (\mathcal{D}^*)

7. Conclusion

In this work, we attempted to give a first insight into the possible capacity improvement in the local radio access arising from the exploitation of the cognitive MIMO radio paradigm. The game-inspired approach we have proposed exploits the cognitive capabilities of the overall AN to dynamically perform both adaptive spatial-beamforming at the radios and MAI-mitigation at the AP. The reported numerical results support the conclusion that the

cognitive SDMA policy is able to outperform the more conventional no cognitive strategies based on orthogonal access, requiring neither peer-to-peer cooperation among the accessing radios nor radio synchronization.

8. References

- Altman, E.; Basar, T. & Srikant, R. (2002). Nash equilibria for combined flow control and routing in networks: asymptotic behaviour for a large number of users, *IEEE Trans. on Automatic Control*, Vol. 47, No. 6, June, pp.917–930.
- Altman, E. & Altman, Z. (2003). S-modular games and power control in wireless networks, *IEEE Trans. on Automatic Control*, Vol. 48, No. 5, May, pp.839–842.
- Baccarelli, E. & Biagi, M. (2003). Optimized power allocation and signal shaping for interference-limited multi-antenna 'ad-hoc networks', *Proc. of PWC 2003*, Sept., pp.138–152.
- Baccarelli, E. & Biagi, M. (2004). Power-allocation policy and optimized design of multiple-antenna systems with imperfect channel estimation, *IEEE Trans. on Vehicular Technology*, Vol. 53, No.1, January, pp.136–145.
- Baccarelli, E.; Biagi, M.; Pelizzoni, C.; Cordeschi, N. & Garzia, F. (2005). When does interference not reduce capacity in multi-antenna networks?, *Proc. of IEEE Signal Processing Advances in Wireless Communications*, pp.298–302.
- Baccarelli, E.; Biagi, M.; Pelizzoni, C. & Cordeschi, N. (2007). Optimized power-allocation for multi-antenna systems impaired by multiple access interference and imperfect channel-estimation, *IEEE Trans. on Vehic. Techn.*, Vol. 56, No. 5, Sept., pp.3089–3015.
- Biagi, M. (2006). Cross-layer design of multi-antenna 4G-WLAN, *PhD dissertation* available at <http://infocom.uniroma1.it/~biagi>.
- Butler, J.M. & Webb, W.T. (2006). An implementation of spectrum usage rights for liberalization of the radio spectrum, *Journal of Communication and Networks*, Vol. 8, No. 2, June, pp.163–168.
- Chow, C.T.; Shankar, S.; Kim, H. & Shin, K.G. (2007). What and how much to gain by spectrum agility?, *IEEE Journal of Sel. Areas in Comm.*, Vol. 25, No. 3, Apr., pp.576–588.
- Cordiero, C.; Challapali, K.; Birru, D. & Shankar, S. (2005). IEEE 802.22: the first world wide standard for cognitive radio, *IEEE DySPAN Conf. Proceedings*.
- DARPA (2001). Program available (vision RFC) at http://www.darpa.mil/ato/programs/XG/rfc_vision.pdf.
- Fattahi, A.; Fu, F.; Schaar, M.v.d. & Paganini, F. (2007). Mechanism-based resource allocation for multimedia transmission over spectrum agile wireless networks, Apr., *IEEE JSAC*, Vol. 25, No. 3, pp.601–612.
- FCC Notice of Proposed Rulemaking and Order (2003). Facilitating opportunities for flexible, efficient and reliable spectrum use employing cognitive radio technologies, *ET Docket*, Dec., No. 03–108.
- Fudenberg, D. & Tirole, J. (1991). *Game Theory*, MIT Press.
- Gallagher, R.G. (1968). *Information Theory and Reliable Communication*, Wiley.
- Glisic, S. (2006). *Advanced Wireless Networks: 4G Technologies*, Wiley.
- Goodman, D. & Mandayam, N. (2000). Power-control for wireless data, *IEEE Personal Communications*, April, pp.48–54.

- Haykin, S. (2005). Cognitive radio: brain-empowered wireless communications, *IEEE Journal of Select. Areas in Comm.*, Feb., Vol. 23, No. 1, pp.201–220.
- IEEE 802.22 (2005). working group available at website <http://www.ieee802.org/22>.
- Kannan, R. & Iyengar, S.S. (2004). Game-theoretic models for reliable path-length and energy constrained routing with data aggregation in wireless sensor networks, *IEEE Journal on Sel. Areas in Comm.*, June, Vol. 22, No. 6, pp.1141–1150.
- Lee, P.K. (2001). Joint frequency hopping and adaptive spectrum exploitation, *IEEE MILCOM 2001*, Vol. 1, pp.566–570.
- MacKenzie, A.B. & Wicker, S.B. (2001). Game Theory in communications: motivation, explanation and application to power control, *GLOBECOM 2001*, pp.821–825.
- Mangold, S.; Zhong, Z.; Challapali, K. & Chow, C.T. (2004). Spectrum agile radio: radio resource measurements for opportunistic spectrum usage, *Proc. of GLOBECOM '04*, Dec., Vol. 6, pp.3467–3471.
- Mitola, J. (1999). Cognitive radio for flexible mobile multimedia communications, *Proc. of MoMuC'99*, Nov., pp.3–10.
- Palomar, D.P.; Cioffi, J.M. & Lagunas, M.A. (2003). Uniform power-allocation in MIMO channels: a game-theoretic approach, *IEEE Trans. on Inform. Theory*, July, Vol. 49, No. 7, pp.1707–1727.
- Paulraj, A.; Nabar, E. & Gore, D. (2003). *Introduction to Space-Time Wireless Communications*, Cambridge University Press.
- Poor, H.V. (1994). An introduction to signal detection and estimation, *Springer Texts in Electrical Engineering*.
- Saraydar, C.; Mandayanan, N.B. & Goodman, D.J. (2002). Efficient power control via pricing in wireless data networks, *IEEE Trans. on Comm.*, Feb., Vol. 50, No. 2, pp.291–303.
- Shad, F.; Todd, T.D.; Kezys, V. & Litva, J. (2001). Dynamic slot allocation (DSA) in indoor SDMA/TDMA using a smart antenna base station, *IEEE/ACM Trans. on Networking*, Feb., Vol. 9, No. 1, pp.69–81.
- Sung, C. & Wong, W. (2003). A non-cooperative power-control frame for multirate CDMA data networks, *IEEE Trans on Wireless Comm.*, Jan., Vol. 2, No. 1, pp.186–219.
- Virapanicharoen, J. & Benjpolakaul, W. (2004). Fair-efficient guard bandwidth coefficients selection in call admission control for mobile communications using game-theoretic framework, *IEEE ICC 2004*, June, Vol. 1, pp.80–84.
- Wang, Q. & Brown, T.X. (2007). Public safety and commercial spectrum sharing via network pricing and admission control, *IEEE Journal of Sel. Areas in Comm.*, April, Vol. 25, No. 3, pp.622–632.
- Xing, Y.; Chandramouli, R. & Cordeiro, C. (2007). Price dynamics in competitive agile spectrum access markets, *IEEE Journal of Sel. Areas in Comm.*, April, Vol. 25, No. 3, pp.613–621.
- Zheng, H. & Cao, L. (2005). Device-centric spectrum management, *Proc. of IEEE Intern. Symp. on Dynamic Spectr. Acc. Net. (SySPAN) 2005*, Nov., pp.56–65.



Cognitive Radio Systems

Edited by Wei Wang

ISBN 978-953-307-021-6

Hard cover, 340 pages

Publisher InTech

Published online 01, November, 2009

Published in print edition November, 2009

Cognitive radio is a hot research area for future wireless communications in the recent years. In order to increase the spectrum utilization, cognitive radio makes it possible for unlicensed users to access the spectrum unoccupied by licensed users. Cognitive radio let the equipments more intelligent to communicate with each other in a spectrum-aware manner and provide a new approach for the co-existence of multiple wireless systems. The goal of this book is to provide highlights of the current research topics in the field of cognitive radio systems. The book consists of 17 chapters, addressing various problems in cognitive radio systems.

How to reference

In order to correctly reference this scholarly work, feel free to copy and paste the following:

E. Baccarelli, M. Biagi, N. Cordeschi, T. Patriarca and V. Polli (2009). A Competitive Approach for Designing Multi-Antenna Cognitive Access Networks, Cognitive Radio Systems, Wei Wang (Ed.), ISBN: 978-953-307-021-6, InTech, Available from: <http://www.intechopen.com/books/cognitive-radio-systems/a-competitive-approach-for-designing-multi-antenna-cognitive-access-networks>

INTECH
open science | open minds

InTech Europe

University Campus STeP Ri
Slavka Krautzeka 83/A
51000 Rijeka, Croatia
Phone: +385 (51) 770 447
Fax: +385 (51) 686 166
www.intechopen.com

InTech China

Unit 405, Office Block, Hotel Equatorial Shanghai
No.65, Yan An Road (West), Shanghai, 200040, China
中国上海市延安西路65号上海国际贵都大饭店办公楼405单元
Phone: +86-21-62489820
Fax: +86-21-62489821

© 2009 The Author(s). Licensee IntechOpen. This chapter is distributed under the terms of the [Creative Commons Attribution-NonCommercial-ShareAlike-3.0 License](https://creativecommons.org/licenses/by-nc-sa/3.0/), which permits use, distribution and reproduction for non-commercial purposes, provided the original is properly cited and derivative works building on this content are distributed under the same license.

IntechOpen

IntechOpen